Analysis of Sandwich Beams With a Compliant Core and With In-Plane Rigidity—Extended High-Order Sandwich Panel Theory Versus Elasticity

Catherine N. Phan
Doctoral Student and Graduate Research Assistant
School of Aerospace Engineering,
Georgia Institute of Technology,
Atlanta, GA 30332-0150

Yeoshua Frostig
Professor
Faculty of Civil and Environmental Engineering,
Department of Structural Engineering and Construction Management,
Technion Israel Institute of Technology,
Haifa 32 000, Israel

George A. Kardomateas
Professor
School of Aerospace Engineering,
Georgia Institute of Technology,
Atlanta, GA 30332-0150

A new one-dimensional high-order theory for orthotropic elastic sandwich beams is formulated. This new theory is an extension of the high-order sandwich panel theory (HSAPT) and includes the in-plane rigidity of the core. In this theory, in which the compressibility of the soft core in the transverse direction is also considered, the displacement field of the core has the same functional structure as in the high-order sandwich panel theory. Hence, the transverse displacement in the core is of second order in the transverse coordinate and the in-plane displacements are of third order in the transverse coordinate. The novelty of this theory is that it allows for three generalized coordinates in the core (the axial and transverse displacements at the centroid of the core and the rotation at the centroid of the core) instead of just one (midpoint transverse displacement) commonly adopted in other available theories. It is proven, by comparison to the elasticity solution, that this approach results in superior accuracy, especially for the cases of stiffer cores, for which cases the other available sandwich computational models cannot predict correctly the stress fields involved. Thus, this theory, referred to as the "extended high-order sandwich panel theory" (EHSAPT), can be used with any combinations of core and face sheets and not only the very "soft" cores that the other theories demand. The theory is derived so that all core/face sheet displacement continuity conditions are fulfilled. The governing equations as well as the boundary conditions are derived via a variational principle. The solution procedure is outlined and numerical results for the simply supported case of transverse distributed loading are produced for several typical sandwich configurations. These results are compared with the corresponding ones from the elasticity solution. Furthermore, the results using the classical sandwich model without shear, the first-order shear, and the earlier HSAPT are also presented for completeness. The comparison among these numerical results shows that the solution from the current theory is very close to that of the elasticity in terms of both the displacements and stress or strains, especially the shear stress distributions in the core for a wide range of cores. Finally, it should be noted that the theory is formulated for sandwich panels with a generally asymmetric geometric layout.
[DOI: 10.1115/1.4005550]

Introduction

Typical sandwich panels consist of two stiff metallic or composite thin face sheets separated by a soft/stiff honeycomb or foam thick core of low/high density. This configuration gives the sandwich material system high stiffness and strength with little resultant weight penalty and high-energy absorption capability related to the application of sandwich structures in the construction of aerospace vehicles, naval vehicles, wind turbines, and civil infrastructure. Most of the studies in sandwich panels neglect the transverse deformation of the core as mentioned in a few textbooks [1–3]. The core of a sandwich structure is considered as infinitely rigid in the thickness direction and only its shear stresses are taken into account while the in-plane stresses are neglected as a result of its low rigidity in this direction relative to that of the face sheets. This assumption may be adequate in the analysis of sandwich structural response to a static loading or even to a dynamic loading of long-duration or for cores made of a high-strength metallic honeycomb or similar. However, recent studies [4] have shown significant core transverse deformation/strain in a sandwich structure subject to impulsive loading or localized loads or in the vicinity of abrupt changes in the layout of a sandwich panel. Consideration of the core compressibility implies that the displacements of the upper and lower face sheets may not be identical. Another important issue is the accurate representation of the core shear, which is a key component in sandwich analyses, since cores are typically of very low modulus and thus transverse shear has a significant influence on the structural behavior.

The earliest models of sandwich analysis are the classical or first-order shear models which assume that the core is infinitely rigid (incompressible) in its transverse direction, its in-plane rigidity is neglected, and it has only shear resistance. In general, they are based on the Euler–Bernoulli and Timoshenko beam theories with modulus-weighted stiffnesses. Though these models are simple, their application is most acceptable when the sandwich core is stiff vertically and statically loaded. In general, in modern sandwich panels with cores of foam type, the core is flexible in all directions. Hence the assumption of a stiff core in the vertical direction is violated but the assumption of negligible in-plane stresses is still valid due to its low in-plane rigidity with respect to

Contributed by Applied Mechanics of ASME for publication in the JOURNAL OF APPLIED MECHANICS. Manuscript received June 27, 2010; final manuscript received September 29, 2011; accepted manuscript posted January 31, 2012; published online May 8, 2012. Assoc. Editor: Anthony Waas.

that of the face sheets. Three fairly recent computational models [5–7] consider transverse compressibility in the core. In particular, Frostig et al. [5] proposed a theory for sandwich panels in which the resulting shear strain in the core is constant and the resulting transverse normal strain in the core is linear in z as a result of the assumption that the in-plane rigidity of the core is negligible. Hohe et al. [6] developed a model for sandwich plates in which the transverse normal strain is constant along the transverse coordinate, z, and the shearing strains are first order in z. Li and Kardomateas [7] explored a higher order theory for plates in which the transverse normal strain in the core is of third order in z, and the shear strains in the core are of fourth order in z. Under some circumstances, such as improvement of impact rigidity of the sandwich panel or introduction of in-plane loads into the core, the effect of the in-plane rigidity of the core should be considered, see the work of Frostig [8] that suggested a computational model that takes into account the in-plane rigidity of the core for sandwich panels for stretchable electronic applications.

The accuracy of any of these models can be readily assessed if an elasticity solution exists. Indeed, Pagano [9] presented the three-dimensional elasticity solution for a laminated or sandwich beam for the case of a positive discriminant of the quadratic characteristic equation, which is formed from the orthotropic material constants, and only when these two real roots are positive. The isotropic case, in which there are two equal real roots, was also outlined. Recently, Kardomateas and Phan [10] extended the Pagano [9] solution to the case of (i) negative discriminant, which results in two complex conjugate roots of the quadratic equation, and (ii) positive discriminant but with real negative roots. The case of a negative discriminant is actually frequently encountered in sandwich construction where the orthotropic core is stiffer in the transverse than the in-plane directions. Results from this elasticity solution showed that the core transverse shear is nearly constant for the very soft cores, but it acquires a pronounced distribution, nearly parabolic, as the stiffness of the core increased. The transverse normal strain in the core was found to be nearly linear in z. It should be mentioned that elasticity solutions that address the complex roots for the two-dimensional case (plate) have already been presented by Zenkour [11] and Demasi [12]; however in the present paper, we are dealing with a beam (one-dimensional) configuration.

In this paper, an extension of the HSAPT is presented for a sandwich beam that allows for the transverse shear distribution in the core to acquire the proper distribution as the core stiffness increases as a result of non-negligible in-plane stresses in the core. Thus, this theory is valid for weak or stiff cores. The theory assumes a transverse displacement in the core that varies as a second-order equation in z, and an axial displacement that is of third order in z, following the displacement distributions of the HSAPT model, see Frostig et al. [5]. However, the novelty of this theory is that it allows for three generalized coordinates in the core (the axial and transverse displacements at the centroid of the core and the rotation at the centroid of the core) instead of just one (midpoint transverse displacement) commonly adopted in other available theories. The theory is formulated for a sandwich panel with a general layout. The major assumptions of the theory are as follows: (1) the face sheets satisfy the Euler–Bernoulli assumptions, and their thicknesses are small compared with the overall thickness of the sandwich section; they can be made of different materials and can have different thicknesses; they undergo large displacements with moderate rotations. (2) The core is compressible in the transverse and axial directions (transverse displacement is second order in z and axial displacement is third in z); it has in-plane, transverse, and shear rigidities; it undergoes large displacements but with kinematic relations of small deformations due to its low in-plane rigidity as compared with that of the face sheets. (3) The face sheets and core are perfectly bonded at their interfaces.

Results will be presented in comparison with the elasticity and the first-order shear deformation (FOSD) theory and the HSAPT.

It should be noted that the purpose of the paper is not to present a general purpose model for a layer-wise panel as in the work of Demasi [13]. For a survey and review of various plate theories (zigzag, layerwise, mixed, etc.), see Carrera and Brischetto [14] and Carrera [15]. Instead, our paper is aimed to present an extension of the HSAPT model and to demonstrate that this extended theory yields accurate results when compared with elasticity solutions for a wide range of skin over core stiffness ratios. Moreover, benchmarks for two-dimensional (plate/shell) theories have been presented by Carrera and Demasi [16]. These benchmarks can be useful in future extensions of our theory to the two-dimensional (plate/shell) configuration; please note that in the present paper, we deal with the one-dimensional configuration (beam) case.

Derivation of the Extended High-Order Sandwich Panel Theory

Figure 1 shows a sandwich panel of length a with a core of thickness $2c$ and top and bottom face sheet thicknesses f_t and f_b, respectively. A Cartesian coordinate system (x, y, z) is defined at one end of the beam and its origin is placed at the middle of the core. Only loading in the $x-z$ plane is considered to act on the beam, which solely causes displacements in the x and z directions designated by u and w, respectively. The superscripts t, b, and c shall refer to the top face sheet, bottom face sheet, and core, respectively. The subscript 0 refers to the middle surface of the corresponding phase. We should also note that in our formulation, the rigidities and all applied loadings are per unit width.

The displacement field of the top and bottom face sheets is assumed to satisfy the Euler–Bernoulli assumptions: Therefore, the displacement field for the top face sheet, $c \le z \le c + f_t$, is

$$w^t(x,z) = w_0^t(x); \quad u^t(x,z) = u_0^t(x) - \left(z - c - \frac{f_t}{2}\right) w_{0,x}^t(x) \tag{1a}$$

and for the bottom face sheet, $-(c+f_b) \le z \le -c$

$$w^b(x,z) = w_0^b(x); \quad u^b(x,z) = u_0^b(x) - \left(z + c + \frac{f_b}{2}\right) w_{0,x}^b(x) \tag{1b}$$

The only nonzero strain in the faces is the axial strain, which in the general nonlinear case (necessary, for example, for buckling) is

$$\epsilon_{xx}^{t,b}(x,z) = u_{,x}^{t,b}(x,z) + \frac{1}{2}\left[w_{0,x}^{t,b}(x)\right]^2 \tag{1c}$$

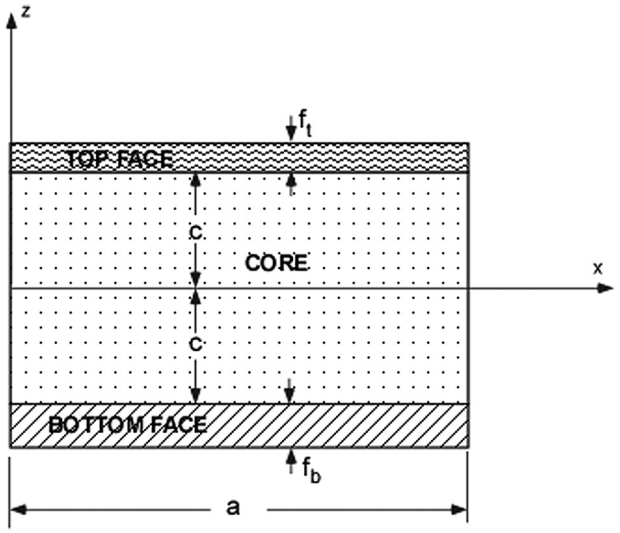

Fig. 1 Definition of the sandwich configuration

If a linear analysis is pursued, the second (squared) term in Eq. (1*c*) is neglected.

While the face sheets can change their length only longitudinally, the core can change its height and length. The displacement fields considered for the core follow the resulting fields that are in the HSAPT model, see Frostig et al. [5], and they read

$$w^c(x,z) = w_0^c(x) + w_1^c(x)z + w_2^c(x)z^2 \tag{2a}$$

$$u^c(x,z) = u_0^c(x) + \phi_0^c(x)z + u_2^c(x)z^2 + u_3^c(x)z^3 \tag{2b}$$

In these equations, w_0^c and u_0^c are the transverse and in-plane displacements, respectively, and ϕ_0^c is the slope at the centroid of the core, while w_1^c, w_2^c and u_2^c, u_3^c are the transverse and in-plane unknown functions to be determined by the transverse and the in-plane compatibility conditions applied at the upper, $z=c$, and lower, $z=-c$, face–core interfaces, Equations (1*a*) and (1*b*). Hence, using the compatibility condition in the transverse direction at the upper and the lower face core interfaces (same core and face sheet transverse displacement) yields the following distribution of the transverse displacement:

$$w^c(x,z) = \left(-\frac{z}{2c}+\frac{z^2}{2c^2}\right)w_0^b(x) + \left(1-\frac{z^2}{c^2}\right)w_0^c(x) + \left(\frac{z}{2c}+\frac{z^2}{2c^2}\right)w_0^t(x) \tag{3}$$

The axial displacement of the core, $u^c(x,z)$, is determined through the fulfillment of the compatibility conditions in the in-plane direction, see second equation in Eqs. (1*a*) and (1*b*) at $z=c$ and $-c$ (same core and face sheet axial displacement at the interface). Hence, after some algebraic manipulation, they read

$$u^c(x,z) = z\left(1-\frac{z^2}{c^2}\right)\phi_0^c(x) + \frac{z^2}{2c^2}\left(1-\frac{z}{c}\right)u_0^b + \left(1-\frac{z^2}{c^2}\right)u_0^c + \frac{z^2}{2c^2}\left(1+\frac{z}{c}\right)u_0^t + \frac{f_b z^2}{4c^2}\left(-1+\frac{z}{c}\right)w_{0,x}^b + \frac{f_t z^2}{4c^2}\left(1+\frac{z}{c}\right)w_{0,x}^t \tag{4}$$

Therefore, this theory is in terms of seven generalized coordinates (unknown functions of x): two for the top face sheet, w_0^t, u_0^t, two for the bottom face sheet, w_0^b, u_0^b, and three for the core, w_0^c, u_0^c, and ϕ_0^c.

The strains can be obtained from the displacements using the linear strain–displacement relations. For the core, the transverse normal strain is

$$\epsilon_{zz}^c = \frac{\partial w^c}{\partial z} = \left(\frac{z}{c^2}-\frac{1}{2c}\right)w_0^b - \frac{2z}{c^2}w_0^c + \left(\frac{z}{c^2}+\frac{1}{2c}\right)w_0^t \tag{5}$$

and the shear strain is

$$\gamma_{zx}^c = \frac{\partial u^c}{\partial z} + \frac{\partial w^c}{\partial x} = \left(1-\frac{3z^2}{c^2}\right)\phi_0^c + \left(\frac{z}{c^2}-\frac{3z^2}{2c^3}\right)u_0^b - \left(\frac{2z}{c^2}\right)u_0^c + \left(\frac{z}{c^2}+\frac{3z^2}{2c^3}\right)u_0^t + \left[-\left(\frac{c+f_b}{2c^2}\right)z + \left(\frac{2c+3f_b}{4c^3}\right)z^2\right]w_{0,x}^b + \left(1-\frac{z^2}{c^2}\right)w_{0,x}^c + \left[\left(\frac{c+f_t}{2c^2}\right)z + \left(\frac{2c+3f_t}{4c^3}\right)z^2\right]w_{0,x}^t \tag{6}$$

There is also a nonzero linear axial strain in the core $\epsilon_{xx}^c = \frac{du^c}{dx}$, which has the same structure as Eq. (4) but with the generalized function coordinates replaced by one order higher derivative with respect to x.

In the following, we use the notation $1 \equiv x$, $3 \equiv z$, and $55 \equiv xz$. We assume orthotropic face sheets, thus the nonzero stresses for the faces are

$$\sigma_{xx}^{t,b} = C_{11}^{t,b}\epsilon_{xx}^{t,b}; \quad \sigma_{zz}^{t,b} = C_{13}^{t,b}\epsilon_{xx}^{t,b} \tag{7a}$$

where in terms of the extensional (Young's) modulus, $E_1^{t,b}$, and the Poisson's ratio, $\nu_{31}^{t,b}$, the stiffness constants for a beam are $C_{11}^{t,b} = E_1^{t,b}$ and $C_{13}^{t,b} = \nu_{31}^{t,b}E_1^{t,b}$. Notice that the $\sigma_{zz}^{t,b}$ does not ultimately enter into the variational equation because the corresponding strain $\epsilon_{zz}^{t,b}$ is zero.

We also assume an orthotropic core with stress–strain relations

$$\begin{bmatrix}\sigma_{xx}^c\\ \sigma_{zz}^c\\ \tau_{xz}^c\end{bmatrix} = \begin{bmatrix}C_{11}^c & C_{13}^c & 0\\ C_{13}^c & C_{33}^c & 0\\ 0 & 0 & C_{55}^c\end{bmatrix}\begin{bmatrix}\epsilon_{xx}^c\\ \epsilon_{zz}^c\\ \gamma_{xz}^c\end{bmatrix} \tag{7b}$$

where C_{ij}^c are the stiffness constants for the core, and we have used the notation $1 \equiv x$, $3 \equiv z$, and $55 \equiv xz$. The stiffness matrix with components C_{ij}^c in Eq. (7*b*) is the inverse of the compliance matrix, whose components a_{ij}^c are expressed in terms of the extensional and shear moduli and Poisson's ratio of the core as

$$a_{11}^c = \frac{1}{E_1^c}; \quad a_{13}^c = -\frac{\nu_{31}^c}{E_3^c}; \quad a_{33}^c = \frac{1}{E_3^c}; \quad a_{55}^c = \frac{1}{G_{31}^c} \tag{7c}$$

The governing equations and boundary conditions are derived from the variational principle

$$\delta(U+V) = 0 \tag{8}$$

where U is the strain energy of the sandwich beam and V is the potential due to the applied loading. The first variation of the strain energy per unit width of the sandwich beam is

$$\delta U = \int_0^a \left[\int_{-c+f_b}^{-c}\sigma_{xx}^b\delta\epsilon_{xx}^b dz + \int_{-c}^{c}\left(\sigma_{xx}^c\delta\epsilon_{xx}^c + \sigma_{zz}^c\delta\epsilon_{zz}^c + \tau_{zx}^c\delta\gamma_{zx}^c\right)dz + \int_{c}^{c+f_t}\sigma_{xx}^t\delta\epsilon_{xx}^t dz\right]dx \tag{9a}$$

and the first variation of the external potential per unit width due to several general loading conditions is

$$\delta V = -\int_0^a\left(\tilde{p}^t\delta u_0^t + \tilde{p}^b\delta u_0^b + \tilde{q}^t\delta w_0^t + \tilde{q}^b\delta w_0^b + \tilde{m}^t\delta w_{0,x}^t + \tilde{m}^b\delta w_{0,x}^b\right)dx - \tilde{N}^t\delta u_0^t\Big]_{x=0}^a - \tilde{N}^b\delta u_0^b\Big]_{x=0}^a - \tilde{V}^t\delta w_0^t\Big]_{x=0}^a - \tilde{V}^b\delta w_0^b\Big]_{x=0}^a - \tilde{M}^t\delta w_{0,x}^t\Big]_{x=0}^a - \tilde{M}^b\delta w_{0,x}^b\Big]_{x=0}^a - \left(\int_{-c}^{c}\tilde{n}^c\delta u^c + \tilde{v}^c\delta w^c\right)dz\Big]_{x=0}^a \tag{9b}$$

where $\tilde{p}^{t,b}$ is the distributed in-plane force (along x) per unit width, $\tilde{q}^{t,b}$ is the distributed transverse (along z) force per unit width, and $\tilde{m}^{t,b}$ is the distributed moment unit width on the top and bottom face sheets. Moreover, $\tilde{N}^{t,b}$ is the end axial force per unit width, $\tilde{V}^{t,b}$ is the end shear force per unit width, and $\tilde{M}^{t,b}$ is the end moment per unit width at the top and bottom face sheets, at the ends $x=0,a$. In addition, $\tilde{n}^c$ is the end axial force per unit width and $\tilde{v}^c$ is the end shear force per unit width at the core at the ends $x=0,a$.

In the following, we assume that $\tilde{n}^c$ and $\tilde{v}^c$ are constant. In this case,

$$\int_{-c}^{c}\tilde{n}^c\delta u^c dz = \tilde{n}^c c\left[\frac{1}{3}\left(\delta u_0^b + \delta u_0^t\right) + \frac{4}{3}\left(\delta u_0^c\right) - \frac{f_b}{6}\delta w_{0,x}^b + \frac{f_t}{6}\delta w_{0,x}^t\right] \tag{9c}$$

$$\int_{-c}^{c}\tilde{v}^c\delta w^c dz = \tilde{v}^c c\left(\frac{1}{3}\delta w_0^b + \frac{4}{3}\delta w_0^c + \frac{1}{3}\delta w_0^t\right) \tag{9d}$$

Of course, the theory can admit any variation of $\tilde{n}^c$ and $\tilde{v}^c$ along z; for example, a bending moment on the core would correspond to a

linear variation of $\tilde{n}^c$ with respect to z. However, for most practical purposes, loads are applied to the skins and not the core.

For the sandwich plates made out of orthotropic materials, we can substitute the stresses in terms of the strains from the constitutive relations, Eqs. (7), and then the strains in terms of the displacements and the displacement profiles, Eqs. (1), (2), and (4), and finally apply the variational principle, Eqs. (8) and (9); thus, we can write a set of nonlinear governing differential equations (DEs) in terms of the seven unknown generalized coordinates as follows.

Top face sheet DEs (two nonlinear)

$$\delta u_0^t : -\left(\frac{4}{5}C_{55}^c + \frac{2c^2}{35}C_{11}^c\frac{\partial^2}{\partial x^2}\right)\phi_0^c - \left(\frac{7}{30c}C_{55}^c + \frac{c}{35}C_{11}^c\frac{\partial^2}{\partial x^2}\right)u_0^b - \left(\frac{4}{3c}C_{55}^c + \frac{2c}{15}C_{11}^c\frac{\partial^2}{\partial x^2}\right)u_0^c + \left(\frac{47}{30c}C_{55}^c - \alpha_1^t\frac{\partial^2}{\partial x^2}\right)u_0^t - \left(\alpha_2^b\frac{\partial}{\partial x} - \frac{cf_b}{70}C_{11}^c\frac{\partial^3}{\partial x^3}\right)w_0^b + \left(\beta_1\frac{\partial}{\partial x}\right)w_0^c + \left(\alpha_3^t\frac{\partial}{\partial x} - \frac{3cf_t}{35}C_{11}^c\frac{\partial^3}{\partial x^3}\right)w_0^t = \tilde{p}^t + F_u^t \tag{10a}$$

where F_u^t is the nonlinear term

$$F_u^t = C_{11}^t f_t w_{0,x}^t w_{0,xx}^t \tag{10b}$$

and $\tilde{p}^t$ is the distributed in-plane force (along x) per unit width at the top face.

And

$$\delta w_0^t : \left(\alpha_4^t\frac{\partial}{\partial x} + \frac{c^2 f_t}{35}C_{11}^c\frac{\partial^3}{\partial x^3}\right)\phi_0^c + \left(\alpha_5^t\frac{\partial}{\partial x} + \frac{cf_t}{70}C_{11}^c\frac{\partial^3}{\partial x^3}\right)u_0^b + \left(\alpha_6^t\frac{\partial}{\partial x} + \frac{cf_t}{15}C_{11}^c\frac{\partial^3}{\partial x^3}\right)u_0^c + \left(-\alpha_3^t\frac{\partial}{\partial x} + \frac{3cf_t}{35}C_{11}^c\frac{\partial^3}{\partial x^3}\right)u_0^t + \left(\frac{1}{6c}C_{33}^c + \beta_2\frac{\partial^2}{\partial x^2} - \frac{cf_b f_t}{140}C_{11}^c\frac{\partial^4}{\partial x^4}\right)w_0^b + \left(-\frac{4}{3c}C_{33}^c + \alpha_7^t\frac{\partial^2}{\partial x^2}\right)w_0^c + \left(\frac{7}{6c}C_{33}^c + \alpha_8^t\frac{\partial^2}{\partial x^2} + \alpha_9^t\frac{\partial^4}{\partial x^4}\right)w_0^t = \tilde{q}^t - \tilde{m}_{,x}^t + F_w^t \tag{11a}$$

where F_w^t is the nonlinear term

$$F_w^t = C_{11}^t f_t\left[w_{0,x}^t u_{0,xx}^t + u_{0,x}^t w_{0,xx}^t + \frac{3}{2}(w_{0,x}^t)^2 w_{0,xx}^t\right] \tag{11b}$$

and $\tilde{q}^t$ is the distributed transverse (along z) force per unit width and $\tilde{m}^t$ is the distributed moment per unit width on the top face sheet.

Core DEs (three linear)

$$\delta u_0^c : -\left(\frac{4}{3c}C_{55}^c + \frac{2c}{15}C_{11}^c\frac{\partial^2}{\partial x^2}\right)u_0^b + \left(\frac{8}{3c}C_{55}^c - \frac{16c}{15}C_{11}^c\frac{\partial^2}{\partial x^2}\right)u_0^c - \left(\frac{4}{3c}C_{55}^c + \frac{2c}{15}C_{11}^c\frac{\partial^2}{\partial x^2}\right)u_0^t + \left(\alpha_6^b\frac{\partial}{\partial x} + \frac{cf_b}{15}C_{11}^c\frac{\partial^3}{\partial x^3}\right)w_0^b - \left(\alpha_6^t\frac{\partial}{\partial x} + \frac{cf_t}{15}C_{11}^c\frac{\partial^3}{\partial x^3}\right)w_0^t = 0 \tag{12a}$$

$$\delta\phi_0^c : \left(\frac{8c}{5}C_{55}^c - \frac{16c^3}{105}C_{11}^c\frac{\partial^2}{\partial x^2}\right)\phi_0^c + \left(\frac{4}{5}C_{55}^c + \frac{2c^2}{35}C_{11}^c\frac{\partial^2}{\partial x^2}\right)u_0^b - \left(\frac{4}{5}C_{55}^c + \frac{2c^2}{35}C_{11}^c\frac{\partial^2}{\partial x^2}\right)u_0^t - \left(\alpha_4^b\frac{\partial}{\partial x} + \frac{c^2 f_b}{35}C_{11}^c\frac{\partial^3}{\partial x^3}\right)w_0^b + \left(\beta_3\frac{\partial}{\partial x}\right)w_0^c - \left(\alpha_4^t\frac{\partial}{\partial x} + \frac{c^2 f_t}{35}C_{11}^c\frac{\partial^3}{\partial x^3}\right)w_0^t = 0 \tag{12b}$$

and

$$\delta w_0^c : -\left(\beta_3\frac{\partial}{\partial x}\right)\phi_0^c + \left(\beta_1\frac{\partial}{\partial x}\right)u_0^b - \left(\beta_1\frac{\partial}{\partial x}\right)u_0^t + \left(-\frac{4}{3c}C_{33}^c + \alpha_7^b\frac{\partial^2}{\partial x^2}\right)w_0^b + \left(\frac{8}{3c}C_{33}^c - \frac{16c}{15}C_{55}^c\frac{\partial^2}{\partial x^2}\right)w_0^c + \left(-\frac{4}{3c}C_{33}^c + \alpha_7^t\frac{\partial^2}{\partial x^2}\right)w_0^t = 0 \tag{12c}$$

Bottom face sheet DEs (two nonlinear)

$$\delta u_0^b : \left(\frac{4}{5}C_{55}^c + \frac{2c^2}{35}C_{11}^c\frac{\partial^2}{\partial x^2}\right)\phi_0^c + \left(\frac{47}{30c}C_{55}^c - \alpha_1^b\frac{\partial^2}{\partial x^2}\right)u_0^b - \left(\frac{4}{3c}C_{55}^c + \frac{2c}{15}C_{11}^c\frac{\partial^2}{\partial x^2}\right)u_0^c - \left(\frac{7}{30c}C_{55}^c + \frac{c}{35}C_{11}^c\frac{\partial^2}{\partial x^2}\right)u_0^t + \left(-\alpha_3^b\frac{\partial}{\partial x} + \frac{3cf_b}{35}C_{11}^c\frac{\partial^3}{\partial x^3}\right)w_0^b - \left(\beta_1\frac{\partial}{\partial x}\right)w_0^c + \left(\alpha_2^t\frac{\partial}{\partial x} - \frac{cf_t}{70}C_{11}^c\frac{\partial^3}{\partial x^3}\right)w_0^t = \tilde{p}^b + \hat{F}_u^b \tag{13a}$$

where F_u^b is the nonlinear term

$$F_u^b = C_{11}^b f_b w_{0,x}^b w_{0,xx}^b \tag{13b}$$

and $\tilde{p}^b$ is the distributed in-plane force (along x) per unit width at the bottom face.

And

$$\delta w_0^b : \left(\alpha_4^b\frac{\partial}{\partial x} + \frac{c^2 f_b}{35}C_{11}^c\frac{\partial^3}{\partial x^3}\right)\phi_0^c + \left(\alpha_3^b\frac{\partial}{\partial x} - \frac{3cf_b}{35}C_{11}^c\frac{\partial^3}{\partial x^3}\right)u_0^b - \left(\alpha_6^b\frac{\partial}{\partial x} + \frac{cf_b}{15}C_{11}^c\frac{\partial^3}{\partial x^3}\right)u_0^c - \left(\alpha_5^b\frac{\partial}{\partial x} + \frac{cf_b}{70}C_{11}^c\frac{\partial^3}{\partial x^3}\right)u_0^t + \left(\frac{7}{6c}C_{33}^c + \alpha_8^b\frac{\partial^2}{\partial x^2} + \alpha_9^b\frac{\partial^4}{\partial x^4}\right)w_0^b + \left(-\frac{4}{3c}C_{33}^c + \alpha_7^b\frac{\partial^2}{\partial x^2}\right)w_0^c + \left(\frac{1}{6c}C_{33}^c + \beta_2\frac{\partial^2}{\partial x^2} - \frac{cf_b f_t}{140}C_{11}^c\frac{\partial^4}{\partial x^4}\right)w_0^t = \tilde{q}^b - \tilde{m}_{,x}^b + F_w^b \tag{14a}$$

where F_w^b is the nonlinear term

$$F_w^b = C_{11}^b f_b\left[w_{0,x}^b u_{0,xx}^b + u_{0,x}^b w_{0,xx}^b + \frac{3}{2}(w_{0,x}^b)^2 w_{0,xx}^b\right] \tag{14b}$$

and $\tilde{q}^b$ is the distributed transverse (along z) force per unit width and $\tilde{m}^b$ is the distributed moment per unit width on the bottom face sheet.

In the above expressions, the following constants are defined:

$$\alpha_1^i = \frac{6c}{35}C_{11}^c + f_i C_{11}^i; \quad \alpha_2^i = \frac{1}{30}C_{13}^c + \left(\frac{1}{30} - \frac{7f_i}{60c}\right)C_{55}^c \tag{15a}$$

$$\alpha_3^i = -\frac{11}{30}C_{13}^c + \left(\frac{19}{30} + \frac{47f_i}{60c}\right)C_{55}^c; \quad \alpha_4^i = \frac{4c}{15}C_{13}^c + \left(\frac{4c}{15} + \frac{2f_i}{5}\right)C_{55}^c \tag{15b}$$

$$\alpha_5^i = -\frac{1}{30}C_{13}^c + \left(-\frac{1}{30} + \frac{7f_i}{60c}\right)C_{55}^c; \quad \alpha_6^i = \frac{2}{3}C_{13}^c + \left(\frac{2}{3} + \frac{2f_i}{3c}\right)C_{55}^c \tag{15c}$$

$$\alpha_7^i = -\frac{f_i}{5}C_{13}^c - \left(\frac{2c}{15} + \frac{f_i}{5}\right)C_{55}^c \tag{15d}$$

$$\alpha_8^i = \frac{11f_i}{30}C_{13}^c - \left(\frac{4c}{15} + \frac{19f_i}{30} + \frac{47f_i^2}{120c}\right)C_{55}^c \tag{15e}$$

$$\alpha_9^i = \frac{f_i^3}{12} C_{11}^i + \frac{3cf_i^2}{70} C_{11}^c \tag{15f}$$

and

$$\beta_1 = \frac{2}{5}(C_{13}^c + C_{55}^c) \tag{15g}$$

$$\beta_2 = \frac{f_b + f_t}{60} C_{13}^c + \left(\frac{c}{15} + \frac{f_b + f_t}{60} - \frac{7f_b f_t}{120c}\right) C_{55}^c \tag{15h}$$

$$\beta_3 = \frac{8c}{15}(C_{13}^c + C_{55}^c) \tag{15i}$$

The corresponding boundary conditions (BCs) at $x = 0, a$ read as follows (at each end there are nine boundary conditions, three for each face sheet and three for the core):

Top face sheet BCs (three)

(i) Either $\delta u_0^t = 0$ or

$$\left(\frac{2c^2}{35} C_{11}^c \frac{\partial}{\partial x}\right)\phi_0^c + \left(\frac{c}{35} C_{11}^c \frac{\partial}{\partial x}\right)u_0^b + \left(\frac{2c}{15} C_{11}^c \frac{\partial}{\partial x}\right)u_0^c + \left[\left(\frac{6c}{35} C_{11}^c + f_t C_{11}^t\right)\frac{\partial}{\partial x}\right]u_0^t + \left(\frac{1}{30} C_{13}^c - \frac{cf_b}{70} C_{11}^c \frac{\partial^2}{\partial x^2}\right)w_0^b - \left(\frac{2}{5} C_{13}^c\right)w_0^c + \left(\frac{11}{30} C_{13}^c + \frac{3cf_t}{35} C_{11}^c \frac{\partial^2}{\partial x^2}\right)w_0^t = \tilde{N}^t + \frac{\tilde{n}^c c}{3} + B_u^t \tag{16a}$$

where $\tilde{N}^t$ is the end axial force per unit width at the top face and $\tilde{n}^c$ is the end axial force per unit width at the core (at the end $x = 0$ or $x = a$) and the nonlinear term

$$B_u^t = -\frac{f_t}{2} C_{11}^t (w_{0,x}^t)^2 \tag{16b}$$

(ii) Either $\delta w_0^t = 0$ or

$$-\left[\frac{2(2c + 3f_t)}{15} C_{55}^c + \frac{c^2 f_t}{35} C_{11}^c \frac{\partial^2}{\partial x^2}\right]\phi_0^c + \left[\frac{(2c - 7f_t)}{60c} C_{55}^c - \frac{cf_t}{70} C_{11}^c \frac{\partial^2}{\partial x^2}\right]u_0^b - \left[\frac{2(c + f_t)}{3c} C_{55}^c + \frac{cf_t}{15} C_{11}^c \frac{\partial^2}{\partial x^2}\right]u_0^c + \left[\frac{(38c + 47f_t)}{60c} C_{55}^c - \frac{3cf_t}{35} C_{11}^c \frac{\partial^2}{\partial x^2}\right]u_0^t + \left[\left(\frac{f_b}{60} C_{13}^c - \beta_2\right)\frac{\partial}{\partial x} + \frac{cf_b f_t}{140} C_{11}^c \frac{\partial^3}{\partial x^3}\right]w_0^b - \left(\alpha_7^t \frac{\partial}{\partial x}\right)w_0^c + \left[\left(\frac{11f_t}{60} C_{13}^c - \alpha_8^t\right)\frac{\partial}{\partial x} - \alpha_9^t \frac{\partial^3}{\partial x^3}\right]w_0^t = \tilde{V}^t + \tilde{m}^t + \frac{\tilde{v}^c c}{3} + B_w^t \tag{17a}$$

where B_w^t is the nonlinear term

$$B_w^t = -\frac{f_t}{2} C_{11}^t w_{0,x}^t \left[2u_{0,x}^t + (w_{0,x}^t)^2\right] \tag{17b}$$

and $\tilde{V}^t$ is the end shear force per unit width at the top face and $\tilde{v}^c$ is the end shear force per unit width at the core (at the end $x = 0$ or $x = a$).

(iii) Either $\delta w_{0,x}^t = 0$ or

$$\left(\frac{c^2 f_t}{35} C_{11}^c \frac{\partial}{\partial x}\right)\phi_0^c + \left(\frac{cf_t}{70} C_{11}^c \frac{\partial}{\partial x}\right)u_0^b + \left(\frac{cf_t}{15} C_{11}^c \frac{\partial}{\partial x}\right)u_0^c + \left(\frac{3cf_t}{35} C_{11}^c \frac{\partial}{\partial x}\right)u_0^t + \left(\frac{f_t}{60} C_{13}^c - \frac{cf_b f_t}{140} C_{11}^c \frac{\partial^2}{\partial x^2}\right)w_0^b - \left(\frac{f_t}{5} C_{13}^c\right)w_0^c + \left(\frac{11f_t}{60} C_{13}^c + \alpha_9^t \frac{\partial^2}{\partial x^2}\right)w_0^t = \tilde{M}^t + \frac{\tilde{n}^c cf_t}{6} \tag{18}$$

where $\tilde{M}^t$ is the end moment per unit width at the top face (at the end $x = 0$ or $x = a$).

Core BCs (three)

(i) Either $\delta u_0^c = 0$ or

$$\left(\frac{2c}{15} C_{11}^c \frac{\partial}{\partial x}\right)u_0^b + \left(\frac{16c}{15} C_{11}^c \frac{\partial}{\partial x}\right)u_0^c + \left(\frac{2c}{15} C_{11}^c \frac{\partial}{\partial x}\right)u_0^t - \left(\frac{2}{3} C_{13}^c + \frac{cf_b}{15} C_{11}^c \frac{\partial^2}{\partial x^2}\right)w_0^b + \left(\frac{2}{3} C_{13}^c + \frac{cf_t}{15} C_{11}^c \frac{\partial^2}{\partial x^2}\right)w_0^t = \frac{4\tilde{n}^c c}{3} \tag{19a}$$

(ii) Either $\delta \phi_0^c = 0$ or

$$\left(\frac{16c^3}{105} C_{11}^c \frac{\partial}{\partial x}\right)\phi_0^c - \left(\frac{2c^2}{35} C_{11}^c \frac{\partial}{\partial x}\right)u_0^b + \left(\frac{2c^2}{35} C_{11}^c \frac{\partial}{\partial x}\right)u_0^t + \left(\frac{4c}{15} C_{13}^c + \frac{c^2 f_b}{35} C_{11}^c \frac{\partial^2}{\partial x^2}\right)w_0^b - \left(\frac{8c}{15} C_{13}^c\right)w_0^c + \left(\frac{4c}{15} C_{13}^c + \frac{c^2 f_t}{35} C_{11}^c \frac{\partial^2}{\partial x^2}\right)w_0^t = 0 \tag{19b}$$

(iii) Either $\delta w_0^c = 0$ or

$$C_{55}^c \left[\frac{8c}{15}\phi_0^c - \frac{2}{5}u_0^b + \frac{2}{5}u_0^t + \frac{(2c + 3f_b)}{15} w_{0,x}^b + \frac{16c}{15} w_{0,x}^c + \frac{(2c + 3f_t)}{15} w_{0,x}^t\right] = \frac{4}{3}\tilde{v}^c c \tag{19c}$$

Bottom face sheet BCs (three)

(i) Either $\delta u_0^b = 0$ or

$$-\left(\frac{2c^2}{35}C_{11}^c\frac{\partial}{\partial x}\right)\phi_0^c+\left[\left(\frac{6c}{35}C_{11}^c+f_bC_{11}^b\right)\frac{\partial}{\partial x}\right]u_0^b+\left(\frac{2c}{15}C_{11}^c\frac{\partial}{\partial x}\right)u_0^c+\left(\frac{c}{35}C_{11}^c\frac{\partial}{\partial x}\right)u_0^t-\left(\frac{11}{30}C_{13}^c+\frac{3cf_b}{35}C_{11}^c\frac{\partial^2}{\partial x^2}\right)w_0^b+\left(\frac{2}{5}C_{13}^c\right)w_0^c+\left(-\frac{1}{30}C_{13}^c+\frac{cf_t}{70}C_{11}^c\frac{\partial^2}{\partial x^2}\right)w_0^t=\tilde{N}^b+\frac{\tilde{n}^cc}{3}+B_u^b \tag{20a}$$

where $\tilde{N}^b$ is the end axial force per unit width at the bottom face and the nonlinear term,

$$B_u^b=-\frac{f_b}{2}C_{11}^b(w_{0,x}^b)^2 \tag{20b}$$

(ii) Either $\delta w_0^b = 0$ or

$$-\left[\frac{2(2c+3f_b)}{15}C_{55}^c+\frac{c^2f_b}{35}C_{11}^c\frac{\partial^2}{\partial x^2}\right]\phi_0^c+\left[-\frac{(38c-47f_b)}{60c}C_{55}^c+\frac{3cf_b}{35}C_{11}^c\frac{\partial^2}{\partial x^2}\right]u_0^b+\left[\frac{2(c+f_b)}{3c}C_{55}^c+\frac{cf_b}{15}C_{11}^c\frac{\partial^2}{\partial x^2}\right]u_0^c+\left[\frac{(-2c+7f_b)}{60c}C_{55}^c+\frac{cf_b}{70}C_{11}^c\frac{\partial^2}{\partial x^2}\right]u_0^t+\left[\left(\frac{11f_b}{60}C_{13}^c-\alpha_8^b\right)\frac{\partial}{\partial x}-\alpha_9^b\frac{\partial^3}{\partial x^3}\right]w_0^b-\left(\alpha_7^b\frac{\partial}{\partial x}\right)w_0^c+\left[\left(\frac{f_t}{60}C_{13}^c-\beta_2\right)\frac{\partial}{\partial x}+\frac{cf_bf_t}{140}C_{11}^c\frac{\partial^3}{\partial x^3}\right]w_0^t=\tilde{V}^b+\tilde{m}^b+\frac{\tilde{v}^cc}{3}+B_w^b \tag{21a}$$

where B_w^b is the nonlinear term

$$B_w^b=-\frac{f_b}{2}C_{11}^bw_{0,x}^b[2u_{0,x}^b+(w_{0,x}^b)^2] \tag{21b}$$

and $\tilde{V}^b$ is the end shear force per unit width at bottom face.

(iii) Either $\delta w_{0,x}^b = 0$ or

$$\left(\frac{c^2f_b}{35}C_{11}^c\frac{\partial}{\partial x}\right)\phi_0^c-\left(\frac{3cf_b}{35}C_{11}^c\frac{\partial}{\partial x}\right)u_0^b-\left(\frac{cf_b}{15}C_{11}^c\frac{\partial}{\partial x}\right)u_0^c-\left(\frac{cf_b}{70}C_{11}^c\frac{\partial}{\partial x}\right)u_0^t+\left(\frac{11f_b}{60}C_{13}^c+\alpha_9^b\frac{\partial^2}{\partial x^2}\right)w_0^b-\left(\frac{f_b}{5}C_{13}^c\right)w_0^c+\left(\frac{f_b}{60}C_{13}^c-\frac{cf_bf_t}{140}C_{11}^c\frac{\partial^2}{\partial x^2}\right)w_0^t=\tilde{M}^b-\frac{\tilde{n}^ccf_b}{6} \tag{22}$$

where $\tilde{M}^b$ is the end moment per unit width at the bottom face.

The superscript $\tilde{}$ denotes in the above equations the known external boundary values.

Application of the Extended High-Order Sandwich Panel Theory for a Simply Supported Sandwich Panel

In this section, we shall study the linear response of a simply supported sandwich panel under transversely applied loading of the form

$$\tilde{q}^t(x)=q_0\sin\frac{\pi x}{a} \tag{23}$$

The numerical results for several typical sandwich plate configurations with orthotropic phases will be compared with the results using the elasticity solution [10], the classical model, and the first-order shear model as well as the Frostig et al. high-order sandwich panel theory [5].

In this case, the boundary conditions for $x = 0,\ a$ (Fig. 1) are the three kinematic conditions

$$w_0^t=w_0^b=w_0^c=0 \tag{24}$$

and the right hand sides of the 6 natural boundary conditions in Eqs. (16), (18), (19*a*), (19*b*), (20), and (22) are equal to zero.

All these are satisfied by displacements in the form

$$u_0^t=U_0^t\cos\frac{\pi x}{a};\quad u_0^c=U_0^c\cos\frac{\pi x}{a};\quad \phi_0^c=\Phi_0^c\cos\frac{\pi x}{a};\quad u_0^b=U_0^b\cos\frac{\pi x}{a} \tag{25a}$$

$$w_0^t=W_0^t\sin\frac{\pi x}{a};\quad w_0^c=W_0^c\sin\frac{\pi x}{a};\quad w_0^b=W_0^b\sin\frac{\pi x}{a} \tag{25b}$$

We consider the linear problem, which means that the nonlinear terms $F_{u,w}^{t,b}$ in the governing differential equations and the nonlinear terms $B_w^{t,b}$ in the boundary conditions are neglected.

Substituting Eq. (25) into Eqs. (10)–(14) results in a system of seven linear equations for the seven unknown constants U_0^t, U_0^c, Φ_0^c, U_0^b, W_0^t, W_0^c, W_0^b.

We shall consider sandwich configurations consisting of faces made out of either graphite/epoxy or E-glass/polyester unidirectional composite and core made out of either hexagonal glass-phenolic honeycomb or balsa wood. The moduli and Poisson's ratios for these materials are given in Table 1.

The two face sheets are assumed identical with thickness $f_t = f_b = f = 2$ mm. The core thickness is $2c = 16$ mm. The total thickness of the plate is defined as $h_{tot} = 2f + 2c$ and the length of the beam is $a = 20\ h_{tot}$.

In the following results, the displacements are normalized with

$$w_{\text{norm}}=\frac{3q_0a^4}{2\pi^4E_1^ff^3} \tag{26}$$

and the stresses with q_0.

Plotted in Fig. 2 is the normalized displacement at the top face sheet as a function of x, for the case of graphite/epoxy faces and glass phenolic honeycomb core. In this figure, we also show the predictions of the simple classical beam theory, which does not include transverse shear, as well as the first-order shear theories; for the latter, there are two versions: one that is based only on the

Table 1 Material properties. Moduli data are in GPa.

	Graphite epoxy face	E-glass polyester face	Balsa wood core	Glass phenolic honeycomb core
E_1	181.0	40.0	0.671	0.032
E_2	10.3	10.0	0.158	0.032
E_3	10.3	10.0	7.72	0.300
G_{23}	5.96	3.5	0.312	0.048
G_{31}	7.17	4.5	0.312	0.048
G_{12}	7.17	4.5	0.200	0.013
ν_{32}	0.40	0.40	0.49	0.25
ν_{31}	0.016	0.26	0.23	0.25
ν_{12}	0.277	0.065	0.66	0.25

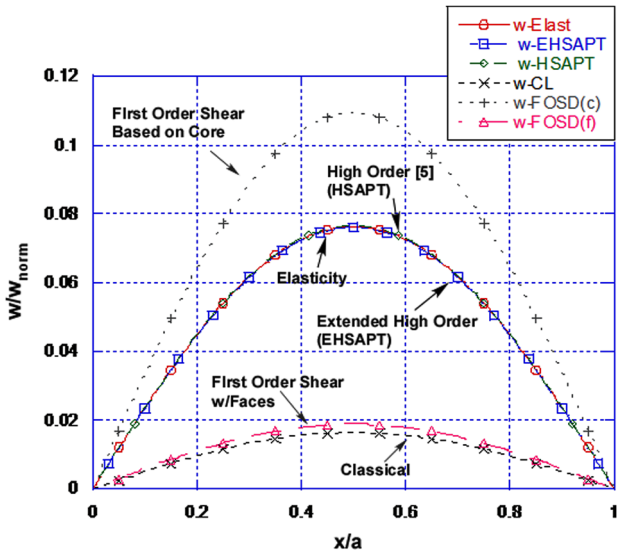

Fig. 2 Transverse displacement, w, at the top, $z = c + f$, for the case of graphite/epoxy faces and glass phenolic honeycomb core

core shear stiffness and one that includes the face sheet stifnesses. Both are outlined in Appendix A. In addition, we show the predictions of the Ref. [5] high-order sandwich panel theory. This theory, which is based on an assumption that the in-plane rigidity of the core is neglected and yields a constant shear stress and zero axial stress in the core, is outlined in Appendix B.

From Fig. 2, we can see that both the classical and first-order shear (both versions) seem to be inadequate. The classical theory is too nonconservative and the first-order shear theory with face sheets included can hardly make a difference. On the other hand, the first-order shear theory where shear is assumed to be carried exclusively by the core is too conservative; this clearly demonstrates the need for higher order theories in dealing with sandwich structures. In this regard, both the Frostig et al. [5] and the present extended high-order theories give a displacement profile which is essentially identical to the elasticity solution. In Fig. 2, we can also readily observe the large effect of transverse shear, which is an important feature of sandwich structures.

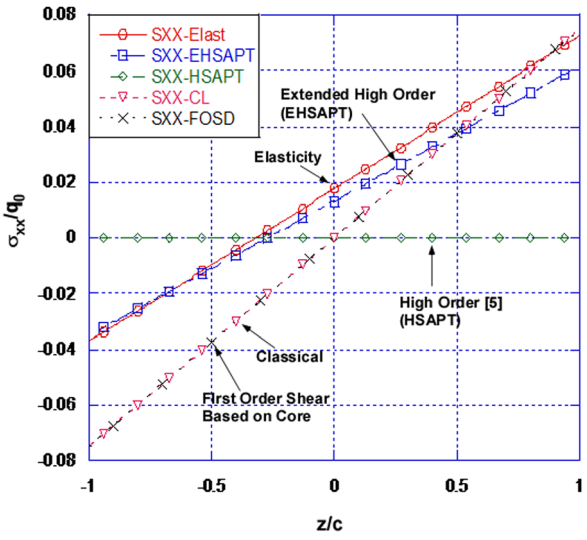

Fig. 3 Through-thickness distribution in the core of the axial stress, σ_{xx}, at $x = a/2$ for the case of graphite/epoxy faces and glass phenolic honeycomb core

The distribution of the axial stress in the core, σ_{xx}, as a function of z at the midspan location, $x = a/2$ (where the bending moment is maximum), is plotted in Fig. 3, again for the case of graphite-epoxy faces and glass phenolic honeycomb core. The present extended high-order theory predicts a stress very close to the elasticity. Note that the Ref. [5] theory neglects the in-plane rigidity of the core that yields a zero axial stress. The classical and first-order shear theories give practically identical predictions but they are in appreciable error by comparison to the elasticity, the error increasing towards the lower end of the core ($z = -c$). All curves are linear. Notice also that for the elasticity and the extended high-order theory, there is not a symmetry with regard to the midline ($z = 0$) unlike the classical and first-order shear theories.

The through-thickness distribution of the transverse normal stress in the core, σ_{zz}, at the midspan location, $x = a/2$, is shown in Fig. 4(*a*) for the case of E-glass/polyester faces and balsa wood core. Only the profiles using elasticity and the Frostig et al. [5] and the extended high-order theories are presented, since the first-order shear theory and the classical theory consider the core incompressible, i.e., zero σ_{zz}. Both high-order theories are

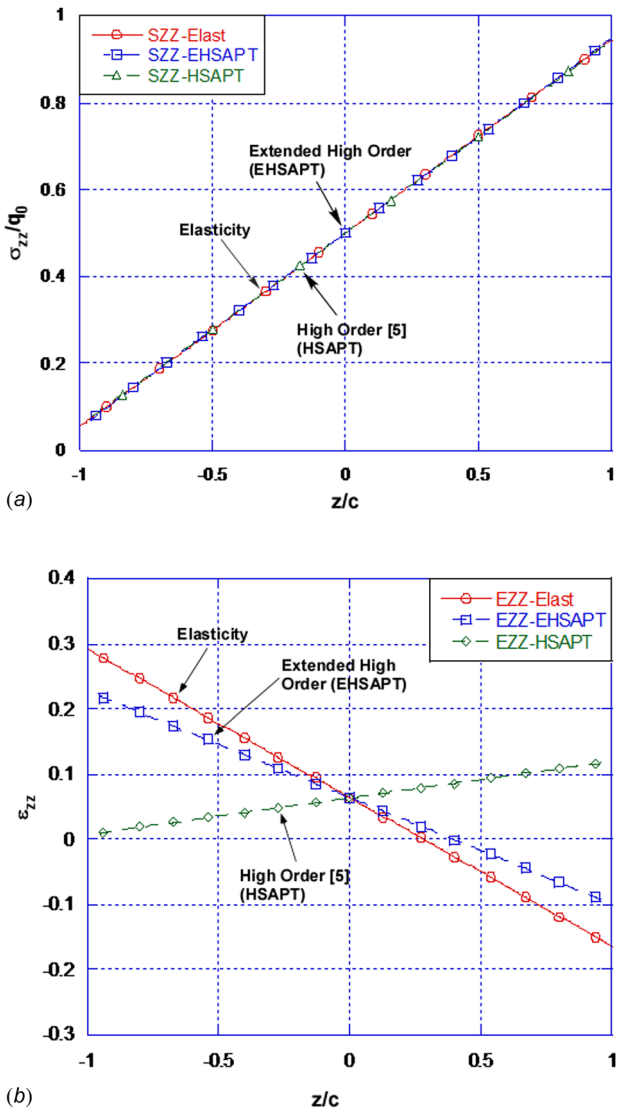

Fig. 4 (*a*) Through-thickness distribution in the core of the transverse normal stress, σ_{zz}, at $x = a/2$ for the case of E-glass/polyester faces and balsa wood core. (*b*) Through-thickness distribution in the core of the transverse normal strain, ϵ_{zz}, at $x = a/2$ for the case of E-glass/polyester faces and balsa wood core.

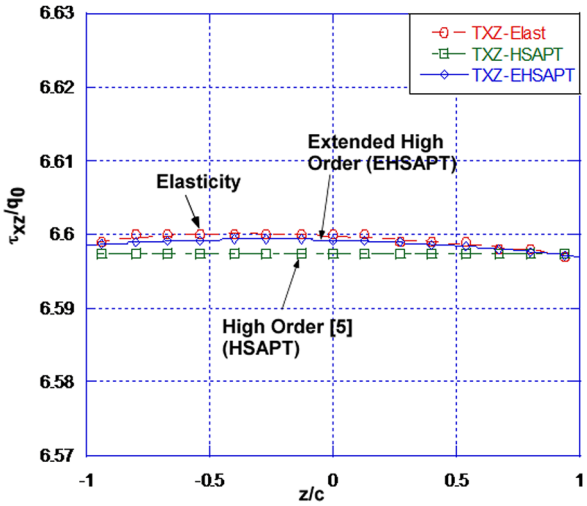

Fig. 5 Through-thickness distribution in the core of the transverse shear stress, τ_{xz}, at $x = a/10$ for the case of graphite/epoxy faces and glass phenolic honeycomb

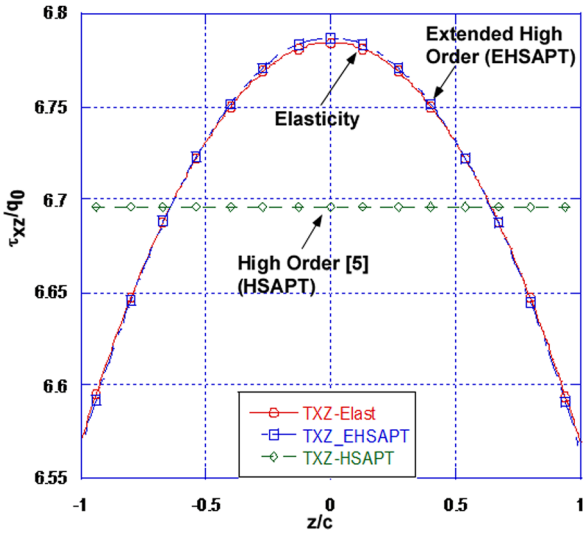

Fig. 6 Through-thickness distribution in the core of the transverse shear stress, τ_{xz}, at $x = a/10$ for the case of E-glass/polyester faces and balsa wood core

practically coinciding with the elasticity curve and all are nearly linear. However, the theories differ when the transverse normal strain is examined in Fig. 4(*b*) with the present extended high-order theory being very close to the elasticity.

Figures 5 and 6 show the through-thickness distribution of the transverse shear stress in the core, τ_{xz}, at $x = a/10$, i.e., near the ends where shearing is expected to be significant, for the cases of graphite/epoxy faces and glass phenolic honeycomb core (Fig. 5) and E-glass/polyester faces and balsa wood core (Fig. 6). For the very soft core case of Fig. 5, the shearing stress is nearly constant and thus for all theories the difference from elasticity is practically negligible. Indeed, the elasticity data show that the range of the shearing stress variation is about 0.05% of the maximum value, i.e., the shearing stress is practically constant. This case of a very soft core would justify the neglect of the in-plane rigidity of the core that is associated with constant shear stresses in the core, made in the Frostig et al. [5] theory. Still, in Fig. 5, one can see that the EHSAPT is practically identical to the elasticity, whereas the HSAPT shows more difference.

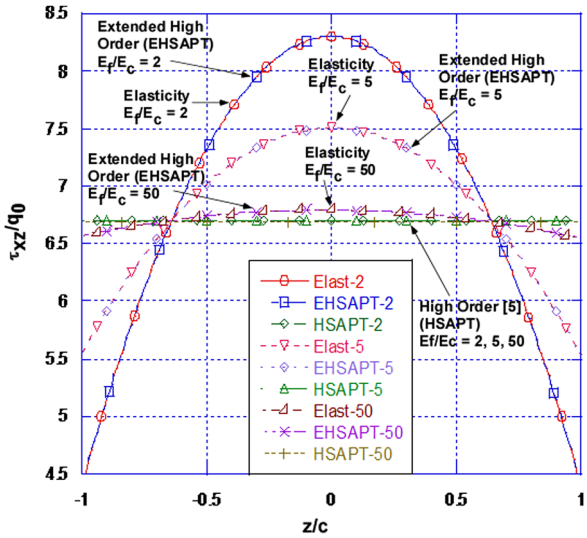

Fig. 7 Through-thickness distribution in the core of the transverse shear stress, τ_{xz}, at $z = a/10$ for the case of isotropic aluminum alloy faces and a wide range of isotropic cores

For the case of the E-glass/polyester faces and balsa wood core, however, the shear stress shows a noticeable distribution (about 5%) through the thickness, which is very nicely captured by the present extended high-order theory, which is practically identical to the Elasticity. For this sandwich configuration, it is obvious that a theory based on a constant shearing stress assumption (HSAPT) would not capture this distribution.

This issue is further explored by considering a sandwich construction in which both the face sheets and the core are isotropic. By varying the moduli ratio, we can accordingly increase the shear stress range in the core. Thus, we assume that the face sheets are made out of isotropic aluminum alloy with $E_f = 100$ GPa and the core is made out of isotropic material having a modulus E_c such that the ratio E_f/E_c assumes the values of 50, 5, and 2. The Poisson's ratios are assumed $\nu_f = \nu_c = 0.30$. Figure 7 shows the shear stress distribution through the thickness. For the moduli ratio of 2, the range is very large, with the maximum over minimum shear stress ratio being about 2. On the contrary, for the moduli ratio of 50, the shear stress range is very small, with the corresponding maximum over minimum shear stress ratio being only about 1.04. The present extended high-order theory is capable of capturing the shear stress profile in all cases, even the most demanding case of $E_f/E_c = 2$ and in all cases is practically identical to the elasticity. On the contrary, a constant shear stress assumption would be applicable only for the large ratios of E_f/E_c.

Carrera and Brischetto [14] have shown that equivalent single layer sandwich plate theories have significant problems in terms of accuracy for very high skin-to-core stiffness ratios. Although we cannot make a direct comparison with their data, since the study in Ref. [14] was done for plates, a similar table as Table 28 in Ref. [14] was made to numerically assess the accuracy of EHSAPT with respect to elasticity for the distributed loading problem shown in this paper. The widely followed FOSD theory is also shown. The material and geometry configurations were taken from Ref. [14]; each face sheet has a thickness $f_t = f_b = f = 0.1$ m, the total core thickness is $2c = 0.8$ m, and the total height $h_{tot} = f_t + f_b + 2c$. A range of beam lengths, a, is examined, as denoted by the length-to-thickness-ratio (LTR) $= a/h_{tot}$; this range of LTRs is {4, 10, 100, 1000}. The core is isotropic with modulus $E_c = 1$ GPa and Poisson's ratio $\nu_c = 0.3$. A range of isotropic faces with modulus E_f and Poisson's ratio $\nu_f = 0.3$ is examined, as denoted by the face-to-core-stiffness-ratio (FCSR) $= E_f/E_c$; this range of FCSRs is $7.3 \times \{10^1, 10^4, 10^6$ and $10^8\}$.

Table 2 Normalized transverse displacements

FCSR	LTR	4	10	100	1000
Midcore ($x = a/2, z = 0$); R = FCSR/LTR					
7.3×10^1	R	18.25	7.3	0.73	0.073
	Elasticity	0.0892	0.0269	0.0148	0.0147
	EHSAPT	0.0907	0.0284	0.0163	0.0162
	FOSD	0.1321	0.0337	0.0152	0.0150
7.3×10^4	R	18,250	7300	730	73
	Elasticity	3.418	2.805	0.1333	0.0161
	EHSAPT	3.725	3.013	0.1351	0.0176
	FOSD	117.09	18.747	0.2023	0.0169
7.3×10^6	R	1.825×10^6	7.3×10^5	7.3×10^4	7.3×10^3
	Elasticity	3.576	3.619	2.811	0.1333
	EHSAPT	3.914	3.973	3.021	0.1351
	FOSD	1.171×10^4	1873.0	18.748	0.2023
7.3×10^8	R	1.825×10^8	7.3×10^7	7.3×10^6	7.3×10^5
	Elasticity	3.577	3.630	3.629	2.811
	EHSAPT	3.916	3.987	3.987	3.021
	FOSD	1.171×10^6	1.873×10^5	1873.0	18.748
Top face ($x = a/2, z = c + f_t/2$); R = FCSR/LTR					
7.3×10^1	R	18.25	7.3	0.73	0.073
	Elasticity	0.0932	0.0270	0.0148	0.0147
	EHSAPT	0.0956	0.0285	0.0163	0.0162
	FOSD	0.1321	0.0337	0.0152	0.0150
7.3×10^4	R	18,250	7300	730	73
	Elasticity	5.098	2.883	0.1333	0.0161
	EHSAPT	5.664	3.108	0.1351	0.0176
	FOSD	117.09	18.747	0.2023	0.0169
7.3×10^6	R	1.825×10^6	7.3×10^5	7.3×10^4	7.3×10^3
	Elasticity	7.244	6.038	2.812	0.1333
	EHSAPT	7.952	6.725	3.022	0.1351
	FOSD	1.171×10^4	1873.0	18.748	0.2023
7.3×10^8	R	1.825×10^8	7.3×10^7	7.3×10^6	7.3×10^5
	Elasticity	7.291	7.263	3.698	2.811
	EHSAPT	7.999	7.981	4.071	3.021
	FOSD	1.171×10^6	1.873×10^5	1873.0	18.748

Table 2 shows the value of the normalized midspan transverse displacement at the midplane ($x = a/2$, $z = 0$) and at the top face sheet ($x = a/2$, $z = c + ft/2$), respectively. The transverse displacements at the midplane and top locations are presented to show the compressibility of the core (i.e., when the two displacements are not equal). The elasticity data in the tables show that sandwich configurations with high FCSR and low LTR combinations exhibit the most compressibility for this particular static problem. For example, for FCSR= 7.3×10^8 and LTR = 4, the top face sheet has about twice as much displacement as that of the midplane. As FCSR gets smaller (i.e., the core and face sheet properties become more similar) and the LTR becomes higher (i.e., the beam becomes longer), the two displacements become practically the same. The tables also show that the FOSD theory is highly inaccurate in predicting transverse displacement for all cases except for the low FCSR and high LTR combinations. On the contrary, with regard to the two transverse displacements, the EHSAPT is consistently close to elasticity with the deviation from elasticity not exceeding 11%; in many cases, the EHSAPT is very accurate (<2% deviation from elasticity). It should be noted that Table 2 only gives transverse displacement data for two locations and do not capture the entire transverse displacement profile through the thickness.

Table 3 shows the midplane normalized shear stress at (x= $a/10$, $z = 0$). The EHSAPT is very accurate for low FCSR and the full range of LTRs, practically coinciding with elasticity; for the more demanding cases of higher FCSRs, the EHSAPT is still quite accurate with the deviation from elasticity not exceeding 10%. On the contrary, the FOSD is inaccurate in predicting shear stress for all cases; for the high FSCRs and low LTRs, the FOSD stress values are, again, many orders of magnitude that of elasticity. This numerical assessment (although not exhaustive since it considers a fixed face-sheet-to-total-thickness ratio $f/h_{tot} = 0.1$ and does not consider orthotropic materials) gives further insight into the accuracy of EHSAPT with respect to elasticity.

Table 3 Normalized shear stress, τ_{xz}/q_0, near the simple support at ($x = a/10$, $z = 0$); R = FCSR/LTR

FCSR	LTR	4	10	100	1000
7.3×10^1	R	18.25	7.3	0.73	0.073
	Elasticity	1.327	3.373	33.828	338.29
	EHSAPT	1.327	3.373	33.828	338.29
	FOSD	1.816	4.541	45.410	454.10
7.3×10^4	R	18,250	7300	730	73
	Elasticity	0.0602	0.7651	32.406	334.88
	EHSAPT	0.0656	0.8217	32.501	334.89
	FOSD	1.8164	4.5410	45.410	454.10
7.3×10^6	R	1.825×10^6	7.3×10^5	7.3×10^4	7.3×10^3
	Elasticity	6.300×10^{-4}	9.890×10^{-3}	7.657	324.05
	EHSAPT	6.890×10^{-4}	1.085×10^{-2}	8.229	325.01
	FOSD	1.816	4.541	45.410	454.10
7.3×10^8	R	1.825×10^8	7.3×10^7	7.3×10^6	7.3×10^5
	Elasticity	6.301×10^{-6}	9.914×10^{-5}	0.0990	76.575
	EHSAPT	6.894×10^{-6}	1.089×10^{-4}	0.1087	82.289
	FOSD	1.816	4.541	45.410	454.10

Conclusions

A extended high-order sandwich beam theory is formulated, which is capable of including the unique features of sandwich construction, i.e., large transverse shear and core compressibility. The significant new feature of this theory is that it allows for three generalized coordinates in the core (the axial and transverse displacements and the rotation at the centroid of the core) instead of one (midpoint transverse displacement) commonly adopted in all other available theories. It also allows for a nonzero axial stress in the core. In this theory, which is derived for a general asymmetric construction, all displacement continuity conditions at the interface of the core with the top and bottom face sheets are enforced. Moreover, the transverse displacement in the core is of second order in the transverse coordinate, z, and the axial displacement in the core is of the third order in z. A comparison to the elasticity solution shows that this extended high-order theory can be used with any combinations of core and face sheets and not only the very "soft" cores that the other high-order sandwich theories demand.

Results have been presented for the case of transverse loading of a simply supported sandwich beam by comparison to the elasticity, the classical sandwich beam theory, the first-order shear theory, and the HSAPT model, see Frostig et al. [5], for different face sheet and core material combinations. The results show that the present extended high-order theory is very close to the elasticity solution in terms of both the displacements and the transverse stress or strain, as well as axial stress through the core, and, in addition, the shear stress distributions in the core for core materials ranging from very soft to almost half the stiffness of the face sheets. In particular, it captures the very large range of core shear stress and the nearly parabolic profile in the cases of cores that are not soft.

Acknowledgment

The financial support of the Office of Naval Research, Grant N00014-07-10373, and the interest and encouragement of the Grant Monitor, Dr. Y. D. S. Rajapakse, are both gratefully acknowledged.

Appendix A: Classical and First-Order Shear theories

Classical Sandwich Beam Theory (Without Shear). The classical sandwich theory assumes that the core is transversely incompressible and the displacement of the top and bottom face sheets and core are the same. The governing differential equation is

$$D_{11}\frac{\partial^4 w(x)}{\partial x^4} = \tilde{q}^t(x) \tag{A1}$$

where D_{11} is the bending stiffness per unit width of the beam.

In the general asymmetric case, the neutral axis of the sandwich section is defined at a distance e from the x-axis (Fig. 1)

$$e(E_1^t f_t + E_1^b f_b) = E_1^t f_t\left(\frac{f_t}{2}+c\right) - E_1^b f_b\left(\frac{f_b}{2}+c\right) \tag{A2a}$$

Therefore, the bending stiffness per unit width, D_{11}, is

$$D_{11} = E_1^t\frac{f_t^3}{12} + E_1^t f_t\left(\frac{f_t}{2}+c-e\right)^2 + E_1^b\frac{f_b^3}{12} + E_1^t f_b\left(\frac{f_b}{2}+c+e\right)^2 \tag{A2b}$$

For the load of Eq. (23), the displacement is expressed as

$$w(x) = W_0\sin\frac{\pi x}{a} \tag{A3}$$

Substituting into Eq. (A1) leads to

$$W_0 = \frac{q_0 a^4}{D_{11}\pi^4} \tag{A4}$$

First-Order Shear Sandwich Panel Theory. For the first-order shear model, if we let ψ be the shear deformation then the governing equations with shear effects can be written as

$$D_{11}\psi_{,xx}(x) - \kappa D_{55}\left[\psi(x) + w_{,x}(x)\right] = 0 \tag{A5}$$

$$\kappa D_{55}\left[\psi_{,x}(x) + w_{,xx}(x)\right] + \tilde{q}^t(x) = 0 \tag{A6}$$

where $\kappa = 5/6$ is the shear correction factor and

$$D_{55} = G_{13}^c(2c) \tag{A7a}$$

In some versions of the first-order shear model, the shear of the face sheets is included, i.e.,

$$D_{55} = G_{13}^c(2c) + G_{13}^t f_t + G_{13}^b f_b \tag{A7b}$$

Setting

$$w(x) = W_0\sin\frac{\pi x}{a}\ ; \quad \psi(x) = \Psi_0\cos\frac{\pi x}{a} \tag{A8}$$

with the load in the same manner as Eq. (23) and substituting in Eqs. (A5) and (A6) leads to

$$\Psi_0 = -\frac{L_{13}}{L_{11}L_{33}-L_{13}^2}q_0\ ; \quad W_0 = \frac{L_{11}}{L_{11}L_{33}-L_{13}^2}q_0 \tag{A9}$$

where

$$L_{11} = D_{11}\frac{\pi^2}{a^2} + \kappa D_{55}\ ; \quad L_{13} = \kappa D_{55}\frac{\pi}{a}\ ; \quad L_{33} = \kappa D_{55}\frac{\pi^2}{a^2} \tag{A10}$$

Appendix B: The Frostig et al. High-Order Sandwich Panel Theory

This theory [5] is expressed in terms of five generalized coordinates, $u_0^t(x)$, $w_0^t(x)$, $u_0^b(x)$, $w_0^b(x)$, and $\tau^c(x)$. The five differential equations, adapted from Frostig et al. (1992) for the present sandwich geometric and coordinate configuration, are as follows:

Top Face Sheet

$$C_{11}^t f_t u_{0,xx}^t(x) - \tau^c(x) = 0 \tag{B1}$$

$$-\frac{C_{33}^c}{2c}w_0^b(x) + C_{11}^t\frac{f_t^3}{12}w_{0,xxxx}^t(x) + \frac{C_{33}^c}{2c}w_0^t(x) - \frac{2c+f_t}{2}\tau_{,x}^c(x) = \tilde{q}^t(x) \tag{B2}$$

Core

$$u_0^b(x) - u_0^t(x) - \frac{2c+f_b}{2}w_{0,x}^b(x) - \frac{2c+f_t}{2}w_{0,x}^t(x) - \frac{(2c)^3}{12C_{33}^c}\tau_{,xx}^c(x) + \frac{2c}{C_{55}^c}\tau^c(x) = 0 \tag{B3}$$

Bottom Face Sheet

$$C_{11}^b f_b u_{0,xx}^b(x) + \tau^c(x) = 0 \tag{B4}$$

$$C_{11}^b\frac{f_b^3}{12}w_{0,xxxx}^b(x) + \frac{C_{33}^c}{2c}w_0^b(x) - \frac{C_{33}^c}{2c}w_0^t(x) - \frac{2c+f_b}{2}\tau_{,x}^c(x) = 0 \tag{B5}$$

By setting the generalized coordinate profiles in the form

$$u_0^{t,b} = U_0^{t,b}\cos\left(\frac{\pi x}{a}\right)\ ; \quad w_0^{t,b} = W_0^{t,b}\sin\left(\frac{\pi x}{a}\right)\ ; \quad \tau^c = T^c\cos\left(\frac{\pi x}{a}\right) \tag{B6}$$

which satisfy the simply supported boundary conditions, and substituting $\tilde{q}^t(x)$ from Eq. (23), we obtain a system of five linear equations for the $U_0^{t,b}$, $W_0^{t,b}$, and T^c.

In this theory, the displacement field of the core depends on the generalized coordinates in the following way:

$$w^c(x,z) = w_0^b(x) + \frac{z+c}{2c}\left[w_0^t(x) - w_0^b(x)\right] - \frac{z^2-c^2}{2C_{33}^c}\tau_{,x}^c(x) \tag{B7}$$

and

$$u^c(x,z) = u_0^b(x) + \frac{z+c}{C_{55}^c}\tau^c(x) - \frac{1}{2C_{33}^c}\left[(z+c)^2 c - \frac{(z+c)^3}{3}\right]\tau_{,xx}^c(x) - \frac{(z+c)^2}{4c}w_{0,x}^t(x) - \left[\frac{f_t}{2} - \frac{(z+c)^2}{4c} + (z+c)\right]w_{0,x}^b(x) \tag{B8}$$

References

[1] Plantema, F. J., 1966, *Sandwich Construction*, Wiley, New York.

[2] Allen, H. G., 1969, *Analysis and Design of Structural Sandwich Panels*, Pergamon, Oxford.

[3] Vinson, J. R., 1999, *The Behavior of Sandwich Structures of Isotropic and Composite Materials*, Technomic Publishing Company, Lancester, PA.

[4] Wang, E., Gardner, N., and Shukla, A., 2009, "The Blast Resistance of Sandwich Composites With Stepwise Graded Cores," Int. J. Solids Struct., **46**(18–19), pp. 3492–3502.

[5] Frostig, Y., Baruch, M.,Vilnay, O., and Sheinman, I., 1992, "High-Order Theory for Sandwich-Beam Behavior With Transversely Flexible Core," J. Eng. Mech., **118**(5), pp. 1026–1043.

[6] Hohe, J., Librescu, L., and Oh, S. Y., 2006, "Dynamic Buckling of Flat and Curved Sandwich Panels With Transversely Compressible Core," Compos. Struct., **74**, pp. 10–24.
[7] Li, R., and Kardomateas, G. A., 2008, "A Nonlinear High Order Core Theory for Sandwich Plates With Orthotropic Phases," AIAA J., **46**(11), pp. 2926–2934.
[8] Frostig, Y., 2010, "On Wrinkling of a Sandwich Panel With a Compliant Core and the Self-Equilibrated Loads," *9th International Conference of a Sandwich Structure 9 (ICSS9)*, G. Ravichandaran, ed., Pasadena, CA, Jun.
[9] Pagano, N. J., 1969, "Exact Solutions for Composite Laminates in Cylindrical Bending," J. Compos. Mater., **3**, pp. 398–411.
[10] Kardomateas, G. A., and Phan, C. N., 2011, "Three Dimensional Elasticity Solution for Sandwich Beams/Wide Plates With Orthotropic Phases: The Negative Discriminant Case," J. Sandwich Struct. Mater., **13**(6), pp. 641–661.
[11] Zenkour, A. M., 2007, "Three-Dimensional Elasticity Solution for Uniformly Loaded Cross-Ply Laminates and Sandwich Plates," J. Sandwich Struct. Mater., **9**, pp. 213–238.
[12] Demasi, L., 2010, "Three-Dimensional Closed Form Solutions and ∞^3 Theories for Orthotropic Plates," Mech. Adv. Mater. Struct., **17**, pp. 20–39.
[13] Demasi, L., 2008, "2D, Quasi 3D and 3D Exact Solutions for Bending of Thick and Thin Sandwich Plates," J Sandwich Struct. Mater., **10**, pp. 271–310.
[14] Carrera, E., and Brischetto, S., 2009, "A Survey With Numerical Assessment of Classical and Refined Theories for the Analysis of Sandwich Plates," Appl. Mech. Rev., **62**, p. 010803.
[15] Carrera, E., 2003, "Historical Review of Zig-Zag Theories for Multilayered Plates and Shells," Appl. Mech. Rev., **56**(3), pp. 287–308.
[16] Carrera, E., and Demasi, L., 2003, "Two Benchmarks to Assess Two-Dimensional Theories of Sandwich, Composite Plates," AIAA J., **41**(7), pp. 1356–1362.